# Quantification of Ink Diffusion in Microcontact Printing with Self-Assembled Monolayers

**ARTICLE** *in* LANGMUIR · JANUARY 2009

Impact Factor: 4.46 · DOI: 10.1021/la802548u · Source: PubMed



**4 AUTHORS**, INCLUDING:

Andreas Larsson
Luleå University of Technology
**56** PUBLICATIONS **979** CITATIONS

SEE PROFILE

Article

# Quantification of Ink Diffusion in Microcontact Printing with Self-Assembled Monolayers

G. Gannon, J. A. Larsson, J. C. Greer, and D. Thompson

*Langmuir*, **2009**, 25 (1), 242-247 • DOI: 10.1021/la802548u • Publication Date (Web): 02 December 2008



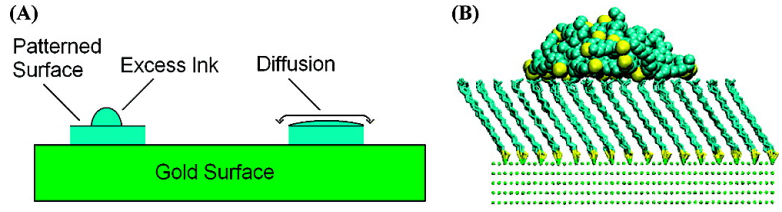


## More About This Article

Additional resources and features associated with this article are available within the HTML version:

- Supporting Information
- Access to high resolution figures
- Links to articles and content related to this article
- Copyright permission to reproduce figures and/or text from this article

View the Full Text HTML

# Quantification of Ink Diffusion in Microcontact Printing with Self-Assembled Monolayers

G. Gannon, J. A. Larsson, J. C. Greer, and D. Thompson*

*Tyndall National Institute, Lee Maltings, Prospect Row, Cork, Ireland*

*Received August 6, 2008. Revised Manuscript Received October 16, 2008*

Spreading of ink outside the desired printed area is one of the major limitations of microcontact printing ($\mu$-CP) with alkanethiol self-assembled monolayers (SAMs) on gold. We use molecular dynamics (MD) computer simulations to quantify the temperature and concentration dependence of hexadecanethiol (HDT) ink spreading on HDT SAMs, modeling 18 distinct printing conditions using periodic simulation cells of ∼7 nm edge length and printing conditions ranging from 7 ink molecules per cell at 270 K to 42 ink molecules per cell at 371K. The computed alkanethiol ink diffusion rates on the SAM are of the same order of magnitude as bulk liquid alkanethiol diffusion rates at all but the lowest ink concentrations and highest temperatures, with up to 20−30 times increases in diffusion rates at the lowest concentration−highest temperature conditions. We show that although alkanethiol surfaces are autophobic, autophobicity is not enough to pin the ink solutions on the SAM, and so any overinking of the SAM will lead to spreading of the printed pattern. Comparison of experimental and calculated diffusion data supports an interpretation of pattern broadening as a mixture of spreading on fully and partially formed SAMs, and the calculated spreading rates establish some of the fundamental limitations of $\mu$-CP in terms of stamp contact time and desired pattern width.

## 1. Introduction

Alkanethiol self-assembled monolayers (SAMs) on gold, specifically the Au(111) surface, have been widely studied since their discovery in the early 1980s.[1] They form well-organized and closely packed structures, characterized by a unit cell,[2] with a tilt angle of 20−30° between the alkanethiol backbone and the plane normal to the gold substrate.[3] The interest in SAMs is due in part to their ease of production but also due to their present and potential application in technologies as diverse as biosensors,[4] corrosion protection,[5] and nanolithography.[6]

Microcontact printing ($\mu$-CP) in particular represents one proven application of SAMs,[7] first described as a method to produce well-defined features (patterns) on gold outside of clean room conditions.[8] One major bottleneck in the technology transfer of $\mu$-CP to routine use in commercial lithography processes however is the lateral spreading of the alkanethiol "ink" molecules used for patterning.[7,9,10] This spreading means the quality of the printed pattern is strongly dependent on the mobility of the ink compound,[11] and so a detailed understanding of ink diffusion on SAMs is crucial to the production of stable, high-resolution nanopatterns.

In the present work, we use atomistic molecular dynamics (MD) computer simulations to probe the atom-scale features of $\mu$-CP using alkanethiol SAMs. Hexadecanethiol (HDT or C16T) is frequently used as the molecular ink in $\mu$-CP with SAMs[12−18] and is the focus of the present work. Our group has previously employed MD simulations to gain insight into the self-assembly and molecular recognition mechanisms underlying nanopatterning with $\beta$-cyclodextrin-terminated alkanethiol SAMs,[19−23] and there exists a substantial literature dealing with computational analysis of SAMs. See, for example, refs 24−31 Of particular relevance here are computational studies of hexadecane molecules interacting with SAMs,[25,26,31] though the issue of molecular diffusion on the SAM was not addressed in these studies. A recent study considering the diffusion of a single tricresyl phosphate molecule

* Corresponding author, damien.thompson@tyndall.ie.

(1) Nuzzo, R. G.; Allara, D. L. *J. Am. Chem. Soc.* **1983**, *105*, 4481–4483.
(2) Camillone, N., III.; Chidsey, C. E. D.; Liu, G.-y.; Scoles, G. *J. Chem. Phys.* **1993**, *98*, 3503–3511.
(3) Porter, M. D.; Bright, T. B.; Allara, D. L.; Chidsey, C. E. D. *J. Am. Chem. Soc.* **1987**, *109*, 3559–3568.
(4) Wink, T.; vanZuilen, S. J.; Bult, A.; vanBennekom, W. P. *Analyst* **1997**, *122*, R43−R50.
(5) Jennings, G. K.; Munro, J. C.; Yong, T. H.; Laibinis, P. E. *Langmuir* **1998**, *14*, 6130–6139.
(6) Sheehan, P. E.; Whitman, L. J. *Phys. Rev. Lett.* **2002**, *88*, 4.
(7) Biebuyck, H. A.; Larsen, N. B.; Delamarche, E.; Michel, B. *IBM J. Res. Dev.* **1997**, *41*, 159–170.
(8) Kumar, A.; Whitesides, G. M. *Appl. Phys. Lett.* **1993**, *63*, 2002–2004.
(9) Delamarche, E.; Schmid, H.; Bietsch, A.; Larsen, N. B.; Rothuizen, H.; Michel, B.; Biebuyck, H. *J. Phys. Chem. B* **1998**, *102*, 3324–3334.
(10) Dameron, A. A.; Hampton, J. R.; Smith, R. K.; Mullen, T. J.; Gillmor, S. D.; Weiss, P. S. *Nano Lett.* **2005**, *5*, 1834–1837.
(11) Balmer, T. E.; Schmid, H.; Stutz, R.; Delamarche, E.; Michel, B.; Spencer, N. D.; Wolf, H. *Langmuir* **2005**, *21*, 622–632.
(12) Zhao, X. M.; Wilbur, J. L.; Whitesides, G. M. *Langmuir* **1996**, *12*, 3257–3264.
(13) Huck, W. T. S.; Yan, L.; Stroock, A.; Haag, R.; Whitesides, G. M. *Langmuir* **1999**, *15*, 6862–6867.
(14) Bietsch, A.; Hegner, M.; Lang, H. P.; Gerber, C. *Langmuir* **2004**, *20*, 5119–5122.
(15) Heule, M.; Schonholzer, U. P.; Gauckler, L. J. *J. Eur. Ceram. Soc.* **2004**, *24*, 2733–2739.
(16) Kraus, T.; Stutz, R.; Balmer, T. E.; Schmid, H.; Malaquin, L.; Spencer, N. D.; Wolf, H. *Langmuir* **2005**, *21*, 7796–7804.
(17) Helmuth, J. A.; Schmid, H.; Stutz, R.; Stemmer, A.; Wolf, H. *J. Am. Chem. Soc.* **2006**, *128*, 9296–9297.
(18) Mack, N. H.; Dong, R.; Nuzzo, R. G. *J. Am. Chem. Soc.* **2006**, *128*, 7871–7881.
(19) Thompson, D.; Larsson, J. A. *J. Phys. Chem. B* **2006**, *110*, 16640–16645.
(20) Thompson, D. *Langmuir* **2007**, *23*, 8441–8451.
(21) Thompson, D. *ChemPhysChem* **2007**, *8*, 1684–1693.
(22) Thompson, D. *J. Phys. Chem. B* **2008**, *112*, 4994–4999.
(23) Cieplak, M.; Thompson, D. *J. Chem. Phys.* **2008**, *128*, 234906–7.
(24) Hautman, J.; Klein, M. L. *J. Chem. Phys.* **1989**, *91*, 4994–5001.
(25) Hautman, J.; Klein, M. L. *Phys. Rev. Lett.* **1991**, *67*, 1763–1766.
(26) Mar, W.; Klein, M. L. *J. Phys.: Condens. Matter* **1994**, *6*, A381−A388.
(27) Mar, W.; Klein, M. L. *Langmuir* **1994**, *10*, 188–196.
(28) Zhang, L. Z.; Goddard, W. A.; Jiang, S. Y. *J. Chem. Phys.* **2002**, *117*, 7342–7349.
(29) Rai, B.; Sathish, P.; Malhotra, C. P.; Pradip; Ayappa, K. G. *Langmuir* **2004**, *20*, 3138–3144.
(30) Vemparala, S.; Karki, B. B.; Kalia, R. K.; Nakano, A.; Vashishta, P. *J. Chem. Phys.* **2004**, *121*, 4323–4330.
(31) Srivastava, P.; Chapman, W. G.; Laibinis, P. E. *Langmuir* **2005**, *21*, 12171–12178.

10.1021/la802548u CCC: $40.75 
Published on Web 12/02/2008

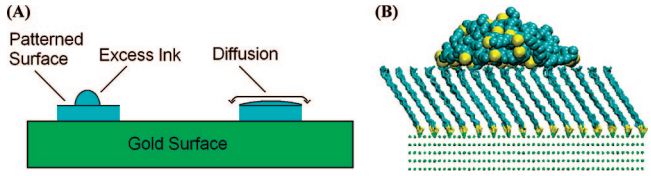


**Figure 1.** (A) Cartoon illustrating the spreading of excess ink in $\mu$-CP, where the Au(111) surface is patterned using alkanethiol "ink" molecules. On the left the pattern contains excess ink and on the right the excess ink has diffused, which will broaden the desired pattern. (B) Representative model of the SAM with excess ink, showing 42 equilibrated hexadecanethiol molecules sitting on a hexadecanethiol SAM at 270 K. Carbon atoms are turquoise, gold atoms are green, and sulfur atoms are yellow.

on top of a SAM[32] is conceptually similar to the present work, although we focus principally on multimolecule diffusion, to compare with $\mu$-CP experiments.

The quantitative data reported herein on alkanethiol spreading will contribute to the design of future $\mu$-CP experiments and may also be used to determine some of the fundamental limitations of $\mu$-CP. Other limitations would include the presence of partially formed monolayers (which do not act as a good resist), grain boundaries in the underlying gold (which may change the rate of SAM formation as well as ink diffusion rates on the SAM surface), and contamination of the ink with low molecular weight "stamp" molecules (for example PDMS monomers and dimers). Focusing on alkanethiol ink spreading, panel a of Figure 1 shows schematically the system we have investigated here. Excess ink is deposited on top of the desired pattern, a consequence of "over-inking" the stamp.[9] In practice some degree of overinking is unavoidable, given the typical few-second contact times[9] and deposited micro/nanoscale patterns.[33] The ink then diffuses, resulting in broadening or "smudging" of the pattern. Using MD simulations, we measure the speed of this diffusion, over a range of ink concentrations and printing temperatures, and describe the balance between molecular clustering and diffusion underlying ink spreading in microcontact printing.

## 2. Methods

**2.1. SAM Model Construction.** We constructed models of the hexadecanethiol (C16T) SAM, based on 224 C16T molecules attached to Au(111). Alkanethiol molecules form a $2\sqrt{3} \times 3$ unit cell[34] on Au(111) with an experimentally measured tilt angle of 30.3° for the structurally similar octadecanethiol (C18T).[35] The on-top position was selected as the attachment site for sulfur on the gold surface,[36] though disagreement exists in the literature about the specific attachment point.[37−39] Regardless of which attachment site is chosen, the lattice constant is the same in all instances. We have tested the dependence of the SAM tilt angle on the fine details of the Au−S−C region by artificially restraining the sulfur atoms and also by removing the gold atoms (see Supporting Information). We obtained a spread of ~3° in the computed time-averaged tilt angles between the three alternate models, similar to the time-averaged standard deviation for each individual model. The on-top position for the sulfur was therefore deemed to be as suitable as the alternatives for the determination of alkanethiol diffusion on top of the SAM.

**2.2. Measuring Bulk Diffusion Coefficients with MD Simulations.** Before measuring ink diffusion on the SAM, we produced reference diffusion data for bulk alkanes and alkanethiols. For the bulk alkane and alkanethiol simulations, 375 molecules of the corresponding alkane or alkanethiol were simulated under a constant number of particles, constant temperature (298 K), and constant pressure (NPT) ensemble conditions. Periodic boundary conditions were applied, and Ewald summation was used to calculate the electrostatic interactions. Temperature was controlled using the Hoover algorithm, and the Leapfrog integrator was used to integrate the equations of motion. We used the CHARMM program version c31b2 for all calculations[40] with standard CHARMM22 force field parameters.[41] Following 700 ps of equilibration (see Supporting Information), molecular dynamics was continued for a further 1.2 ns.

To calculate diffusion coefficients, we used the Einstein diffusion equation

$$D = \frac{1}{2d}\lim_{t\to\infty}\frac{\langle[r(t_0+t) - r(t_0)^2]\rangle}{t} \quad (1)$$

where $D$ is the self-diffusion coefficient and $d$ the dimensionality of the system. The numerator is the mean square displacement, and the angled brackets indicate an ensemble average is to be taken. Care must be taken to ensure that only fully equilibrated data, with many instantaneous positions (MD snapshots) over a long time period are used in calculating $D$.

For example, the diffusion coefficient for bulk HDT over the 1.2 ns of postequilibration dynamics was calculated to be $1.27 \times 10^{-6}$ $cm^2\ s^{-1}$ with a standard deviation of $0.04 \times 10^{-6}$ $cm^2\ s^{-1}$. The diffusion coefficient was calculated as $1.24 \times 10^{-6}$ $cm^2\ s^{-1}$ and $1.29 \times 10^{-6}$ $cm^2\ s^{-1}$ from the first and second 0.6 ns segments, respectively, both within the time-averaged standard deviation in the overall $D$ and illustrating the lack of time dependence in the bulk HDT simulations. As shown in the Supporting Information, all systems in the present study exhibit diffusion behavior that is well-converged with respect to sampling time.

**2.3. Measuring Ink Diffusion on SAMs with MD Simulations.** The C16T SAM was built as described above, with periodic boundary conditions used to approximate the extended system. Simulations were performed in an NVE ensemble, using the CHARMM22 force field[41] supplemented with literature parameters for the Au−S−C region.[42] A range of concentrations of unbound C16T molecules (0, 7, 14, 21, 28, 35, and 42 molecules) were then placed on top of the SAM, as illustrated in Figure 1B. Each system was allowed to equilibrate at a range of temperatures, 270, 331, and 371 ± 3 K, for 1.6 ns followed by 1.8 ns of free dynamics to monitor its structure and dynamics. The very long multinanosecond preparation time was used to allow the excess ink molecules to rearrange freely and migrate away from their initial (arbitrary) positions on the SAM surface. Similar to the bulk simulations above, and as described in detail in the Supporting Information, all computed ink-on-SAM diffusion coefficients are well-converged with respect to time.

## 3. Results and Discussion

**3.1. Control Simulations.** The methodology was validated in a tripartite manner before ink diffusion on the SAM was considered. First diffusion coefficients were calculated for a range of bulk alkanes and compared with experiment. Second bulk

(32) Irving, D. L.; Brenner, D. W. *J. Phys. Chem. B* **2006**, *110*, 15426–15431.
(33) Libioulle, L.; Bietsch, A.; Schmid, H.; Michel, B.; Delamarche, E. *Langmuir* **1999**, *15*, 300–304.
(34) Love, J. C.; Estroff, L. A.; Kriebel, J. K.; Nuzzo, R. G.; Whitesides, G. M. *Chem. Rev.* **2005**, *105*, 1103–1169.
(35) Fenter, P.; Eisenberger, P.; Liang, K. S. *Phys. Rev. Lett.* **1993**, *70*, 2447–2450.
(36) Roper, M. G.; Skegg, M. P.; Fisher, C. J.; Lee, J. J.; Dhanak, V. R.; Woodruff, D. P.; Jones, R. G. *Chem. Phys. Lett.* **2004**, *389*, 87–91.
(37) Fenter, P.; Schreiber, F.; Berman, L.; Scoles, G.; Eisenberger, P.; Bedzyk, M. J. *Surf. Sci.* **1998**, *413*, 213–235.
(38) Gronbeck, H.; Curioni, A.; Andreoni, W. *J. Am. Chem. Soc.* **2000**, *122*, 3839–3842.
(39) Larsson, J. A.; Nolan, M.; Greer, J. C. *J. Phys. Chem. B* **2002**, *106*, 5931–5937.
(40) Brooks, B. R.; Bruccoleri, R. E.; Olafson, B. D.; States, D. J.; Swaminathan, S.; Karplus, M. *J. Comput. Chem.* **1983**, *4*, 187–217.
(41) MacKerell, A. D.; Bashford, D.; Bellott, M.; Dunbrack, R. L.; Evanseck, J. D.; Field, M. J.; Fischer, S.; Gao, J.; Guo, H.; Ha, S.; Joseph-McCarthy, D.; Kuchnir, L.; Kuczera, K.; Lau, F. T. K.; Mattos, C.; Michnick, S.; Ngo, T.; Nguyen, D. T.; Prodhom, B.; Reiher, W. E.; Roux, B.; Schlenkrich, M.; Smith, J. C.; Stote, R.; Straub, J.; Watanabe, M.; Wiorkiewicz-Kuczera, J.; Yin, D.; Karplus, M. *J. Phys. Chem. B* **1998**, *102*, 3586–3616.
(42) Bizzarri, A. R.; Costantini, G.; Cannistraro, S. *Biophys. Chem.* **2003**, *106*, 111–123.

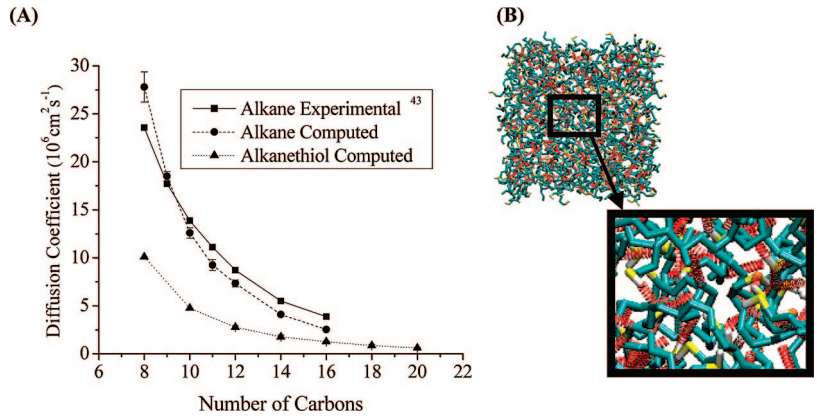


**Figure 2.** (A) Change in bulk diffusion coefficients at 298 K for alkanes and alkanethiols with increasing chain length. Diffusion coefficient values on the *y*-axis have been multiplied by $10^6$. Experimental values were taken from ref 43. Computed diffusion coefficients are from 1.2 ns of equilibrated molecular dynamics, sampling every 10 ps for a total of 120 snapshots with time-averaged standard deviations as shown. The error bars are negligible for all but the shortest-chain runs and represent time-averaged standard deviations. Data points for each data set are connected to guide the eye. (B) Representative MD snapshot showing hydrogen bonds (red) in octanethiol, which impedes diffusion relative to the corresponding alkane. The magnified section clearly shows extensive hydrogen bonding.

diffusion coefficients for a series of alkanethiols were produced. Finally the tilt angle of the SAM was monitored over ~2 ns of free dynamics to assess the structural stability of the SAM model.

There is excellent qualitative and quantitative agreement between measured experimental[43] and our computed diffusion coefficients for alkanes, as shown in Figure 2A. Alkanes were selected due to their structural similarity to alkanethiols and because of the existence of experimental diffusion coefficients.[43] As chain length increases, the diffusion coefficient decreases, in accord with the chemical intuition that longer chains diffuse more slowly than shorter chains. The validation with respect to experiment[43] indicates that the CHARMM22 force field[41] and Einstein diffusion equation (eq 1) accurately model alkane diffusion.

Bulk diffusion coefficients for alkanethiols were also calculated, for which no corresponding experimental values exist in the literature. Figure 2A shows that the alkanes and alkanethiols exhibit a similar dependence on number of carbons and also that the alkanethiols diffuse more slowly than the corresponding alkanes, with this effect particularly pronounced with the shorter chains. This relative decrease in diffusion for the alkanethiols may be understood as a combination of a minor and major effect. The minor effect is the small increase in molecule length as we switch from alkane to alkanethiol; for example, dodecanethiol (C12T) is more comparable to tridecane (C13) than dodecane (C12). More important, and again most pronounced with the shorter chains, is the polarity of the thiol group. The thiol group is chemically similar to the polar OH group, and so transient multimolecular H-bond type complexes form in solution, an example of which from the octanethiol (C8T) MD simulations is shown in Figure 2B. The additional electrostatic interactions for alkanethiols relative to alkanes gives quasi-ordered multimolecular complexes in solution and reduces diffusion (an extreme example of which is seen in salt, for example, guanidinium chloride, solutions[44,45]).

Finally, SAM tilt angles were monitored as a function of time, to test the structural stability of our SAM model prior to the addition of excess ink molecules. The average tilt angle for the C16T SAM over 1.8 ns was 27° at 296 K, with a time-averaged standard deviation of 2.0 from the time lines given in Supporting Information. The computed tilt angle is close to the experimentally

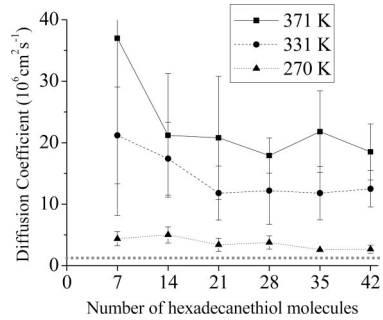


**Figure 3.** The impact of temperature and concentration on hexadecanethiol (HDT) diffusion on the HDT SAM. The error bars represent time-averaged standard deviations and data points for each data set are connected to guide the eye. The *y*-axis has been truncated at 40 × $10^{-6}$cm$^2$ s$^{-1}$; the upper error bar for seven HDT molecules at 369 K extends to 66 × $10^{-6}$cm$^2$ s$^{-1}$. The reference computed diffusion coefficient of 1.27 × $10^{-6}$cm$^2$ s$^{-1}$ for bulk HDT at 298 K is marked as a dashed gray line in the plot.

observed tilt angle of 30.3° for octadecanethiol (C18T) at 303 K.[35] Previous computational studies reported tilt angles of 25° for tridecanethiol (C13T)[30] and 28° for C16T.[24] The tilt angle in our C16T SAM simulations also exhibited the typical variation with temperature,[30] i.e., little change in tilt angle up to 300 K and then an untilting between 300 and 350 K (see Supporting Information).

**3.2. Ink Diffusion as a Function of Temperature and Concentration.** With the validation of the force field and the methodology used to calculate alkanethiol diffusion and model alkanethiol SAMs, an extensive investigation was carried out into the diffusion of C16T ink molecules on the C16T SAM, using three temperatures and six ink concentrations, 18 different printing conditions in all. Figure 1B shows one of the systems studied (42 ink molecules at 270 K). Figure 3 indicates that as the temperature increases, so too does the diffusion coefficient, as expected from kinetic energy considerations. The concentration effect is less pronounced—as the concentration of C16T molecules on the surface increases, the diffusion coefficient generally decreases, up to 21−28 ink molecule concentrations, and then

(43) Tofts, P. S.; Lloyd, D.; Clark, C. A.; Barker, G. J.; Parker, G. J. M.; McConville, P.; Baldock, C.; Pope, J. M. *Magn. Reson. Med.* **2000**, *43*, 368–374.

(44) Mason, P. E.; Neilson, G. W.; Enderby, J. E.; Saboungi, M. L.; Dempsey, C. E.; MacKerell, A. D.; Brady, J. W. *J. Am. Chem. Soc.* **2004**, *126*, 11462–11470.

(45) Gannon, G.; Larsson, J. A.; Greer, J. C.; Thompson, D. *J. Phys. Chem. B* **2008**, *112*, 8906–8911.

*D* becomes insensitive to concentration for up to 42 ink systems. Though there is some overlap in the data at each temperature, the same general trend is observed at the two higher temperatures simulated.

Combining these two observations, it is clear that C16T inks diffuse slowest on the SAM at low temperature and high concentration and fastest at high temperature and low concentration, with approximately an order of magnitude difference in the range of computed ink-on-SAM diffusion coefficients. More generally, the diffusion of C16T on the SAM was shown to be always at least double that of C16T in the reference bulk system (the bulk C16T diffusion coefficient of $1.27 \times 10^{-6}$ cm$^2$ s$^{-1}$ is marked with a dashed gray line in Figure 3). This can be understood when one considers that in the bulk the individual molecules are hindered in their progress in all directions, while on a surface at low concentration the molecules are less hindered. As the concentration of ink on the surface increases, the number of collisions increases and the diffusion coefficient decreases. The higher the concentration of ink on the surface, the closer the conditions and diffusion coefficients resemble bulk diffusion. From Figure 3, it appears that quite low ink concentrations on the order of 1 molecule per nm$^2$ SAM surface area, behave in a near-bulk-like manner, with interink interactions predominating over ink:SAM interactions and giving computed ink-on-SAM *D* values at 270 K approximately twice that of bulk HDT at 298 K.

We also found that the fine details of SAM surface and subsurface alkanethiol packing has little effect on ink diffusion—we computed $D = (22.7 \pm 4.0) \times 10^{-6}$ cm$^2$ s$^{-1}$ for 42 C16T molecules at 371 K with the SAM tilt angle artificially restrained to a low-temperature tilt angle of 32° (see temperature dependence of tilt angle data in Supporting Information). This was very similar to the unrestrained high-temperature system with tilt angle of 5° and $D = (18.5 \pm 4.5) \times 10^{-6}$ cm$^2$ s$^{-1}$ at 371 K (Figure 3).

**3.3. Insights into Ink Diffusion in the Context of $\mu$-CP.** *3.3.1. Ink Spreading Rates as a Function of Ink Concentration.* To give an illustrative example of how the generated diffusion data can be used in the context of $\mu$-CP experiments, the bulk C16T diffusion coefficient of $1.27 \times 10^{-6}$ cm$^2$ s$^{-1}$ (the slowest diffusion coefficient generated for C16T, and corresponding to a very high concentration of ink on the SAM at approximately room temperature) corresponds to $1.27 \times 10^8$ nm$^2$ s$^{-1}$. Therefore, for a printing contact time of 1 s (multiple seconds are normally used[9]) and using eq 2,[46] the average distance traversed within 1 s is 12.7 $\mu$m.

$$\langle x \rangle = 2\left(\frac{Dt}{\pi}\right)^{1/2} \tag{2}$$

$\langle x \rangle$ is the average distance traveled, *D* is the diffusion coefficient, and *t* is time. As this distance is an average value with no directionality, we can interpret it as the radius of a circle and the ink will therefore have covered an area of 506 $\mu$m$^2$ within 1 s. $\mu$-CP patterns typically have submicrometer dimensions.[17,33,47]

The computed diffusion coefficient of C16T on the SAM is about an order of magnitude greater than the value determined experimentally for diffusion of C16T through a PDMS stamp, $(5.3 \pm 0.5) \times 10^{-7}$ cm$^2$ s$^{-1}$.[11] Therefore the more important consideration for limiting pattern smudging is to decrease the amount of ink on the surface by decreasing the stamp:surface contact time. Such dependence of spreading on the surface concentration of ink has been observed experimentally[48] and is at odds with macroscopic autophobic pinning observations.[49] Autophobicity is where a liquid in contact with a surface modifies the chemistry of this surface and the liquid then retracts spontaneously; autophobicity in the present context would mean the alkanethiol ink molecules initially spread on the gold, then as the gold surface is modified by alkanethiol SAM formation, any excess ink will be in contact with an alkanethiol SAM surface rather than a bare gold surface and will spontaneously retract. Autophobic pinning is where an autophobic liquid generates an autophobic surface by reaction to the surface and in which the liquid remains as a drop and does not spread;[49] in the present context this means that the ink would not spread beyond where it was printed due to autophobicity. Note that our purely classical model does not consider the formation of the SAM on Au(111) or the diffusion coefficient associated with it; our system, as represented in Figure 1, deals with just one "transport regime" in $\mu$-CP, that involving ink diffusion on a preformed SAM, one of the more difficult regimes to determine experimentally.[9] In our simulations, the ink molecules show some aggregation on the surface of the SAM, as described in detail below, but nevertheless spread on the surface and diffuse, the intrinsic mobility of the alkanethiol inks overwhelms the (macroscopic) authophobic pinning.

As the diffusion coefficients we determined for ink diffusion on the surface of the SAM are so much faster than the diffusion through the stamp, diffusion on the SAM is arguably the resolution-determining step for $\mu$-CP with C16T SAMs. C16T pattern broadening has been observed experimentally[17] using scanning electron microscopy to occur at a rate of 53 nm in 7 ms or 7.6 $\mu$m s$^{-1}$, similar to the 12.7 $\mu$m s$^{-1}$ predicted here. If we assume the sticking probability of thiol to gold is 1 (as observed in vacuum experiments;[50] note the sticking probability from ethanol is much lower, by a factor of $10^7$ [51]), the rate of advance of the edge of the pattern is determined by the diffusion of ink on the fully formed and partially formed SAM. It is the diffusion of ink on the fully formed perfect SAM that is modeled by our simulations. Diffusion on partially formed SAMs will be impeded relative to diffusion on the more regular fully formed SAM surface (calculated in the present work to be at least 12.7 $\mu$m s$^{-1}$), and so the experimental spreading rate of 7.6 $\mu$m s$^{-1}$ may arise from a combination of ink spreading on fully and partially formed SAMs.

It is interesting to note also that even at the low concentrations investigated here, the surface diffusion coefficients are quite close to the bulk diffusion coefficient of $1.27 \times 10^{-6}$ cm$^2$ s$^{-1}$ at 298 K. The highest computed ink-on-SAM *D* is $37 \times 10^{-6}$ cm$^2$ s$^{-1}$ for seven inks at 371 K, from Figure 3. Simulating vanishingly small ink concentrations, we estimate a diffusion coefficient of $115 \times 10^{-6}$ cm$^2$ s$^{-1}$ for a single C16T molecule on the SAM at 371 K (data not shown), which represents the most unrestricted possible environment for an ink molecule on the SAM, in terms of both low concentration and high temperature. The result is very noisy with typical time-averaged standard deviations of $48 \times 10^{-6}$ cm$^2$ s$^{-1}$ for single-molecule diffusion. Note this increased uncertainty in computed *D* values at lower concentrations is a general result due to the averaging involved in the Einstein diffusion equation (eq 1); see for example our earlier work on bulk diffusion[45] or the work reported in ref 52.

(46) Atkins, P. W. 6th ed.; *Physical Chemistry*; Oxford University Press: Oxford, 1998; p 754.
(47) Menard, E.; Meitl, M. A.; Sun, Y. G.; Park, J. U.; Shir, D. J. L.; Nam, Y. S.; Jeon, S.; Rogers, J. A. *Chem. Rev.* **2007**, *107*, 1117–1160.
(48) Bass, R. B.; Lichtenberger, A. W. *Appl. Surf. Sci.* **2004**, *226*, 335–340.
(49) Biebuyck, H. A.; Whitesides, G. M. *Langmuir* **1994**, *10*, 4581–4587.
(50) Schwartz, P.; Schreiber, F.; Eisenberger, P.; Scoles, G. *Surf. Sci.* **1999**, *423*, 208–224.
(51) Jung, L. S.; Campbell, C. T. *J. Phys. Chem. B* **2000**, *104*, 11168–11178.
(52) Tsai, J.; Gerstein, M.; Levitt, M. *J. Chem. Phys.* **1996**, *104*, 9417–9430.

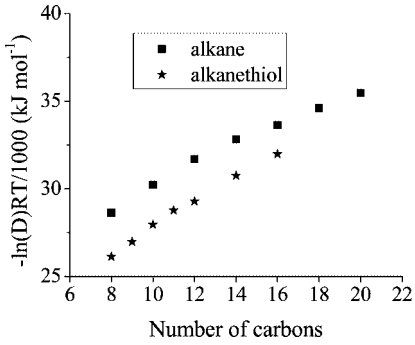


**Figure 4.** Plots of the natural logarithm of the determined diffusion coefficients for the bulk alkane and bulk alkanethiol data sets, multiplied in each case by the negative of the gas constant ($R$) and temperature ($T$) and divided by 1000, vs the number of carbons per molecule. The slope of each plot corresponds to the activation energy per methylene ($CH_2$) group in kJ mol$^{-1}$, as described in the text.

This relatively high single-molecule diffusion (around a hundred times larger than the bulk value at 298 K of $1.27 \times 10^{-6}$ cm$^2$ s$^{-1}$) is however still significantly slower than, for example, alkanes diffusing in nanotubes where unimolecular diffusion under near-frictionless conditions gives velocities on the order of hundreds of meters per second.[53]

*3.3.2. Energetic Barriers to Diffusion.* As well as quantifying the diffusion of HDT molecules on the HDT SAM, we use an Arrhenius type equation (eq 3) to estimate activation energies from the computed diffusion coefficients

$$D = D_\infty \exp(-E_a/RT) \tag{3}$$

where $E_a$ is the activation energy of diffusion per molecule, $D_\infty$ is a constant corresponding to the activation energy of diffusion at infinitely high temperature, and $R$ is the gas constant.

First of all, using eq 3 two activation energy plots were obtained, one for the bulk alkanes and one for the bulk alkanethiols (section 3.1 above). For each data set, plotting the negative of natural logarithm of the bulk diffusion coefficients by the gas constant and temperature divided by 1000 against the number of carbons per molecule and assuming that $D_\infty$ is a constant over the range of molecules simulated, we obtained Figure 4. The slope of the alkane plot yields an activation energy per $CH_2$ group of 0.73 $\pm$ 0.01 kJ mol$^{-1}$ for the bulk alkanes, meaning that the energy required for a linear alkane to diffuse is increased by approximately 0.7 kJ mol$^{-1}$ for each additional $CH_2$ group. Similarly, the activation energy per $CH_2$ obtained for the bulk alkanethiols is 0.56 $\pm$ 0.02 kJ mol$^{-1}$. The value of 0.7 kJ mol$^{-1}$ for each additional $CH_2$ group in the alkane series is very close to the experimentally estimated 0.8 kJ mol$^{-1}$ change in activation energy per $CH_2$ group for the desorption of an alkanethiol from its respective SAM, which was obtained over a range of alkanethiols from decanethiol to docosanethiol.[54] The comparison made here is between the experimental desorption values[54] and the bulk alkane simulations, as the bulk alkane data, rather than bulk alkanethiol data, better represent the bulk hexadecane environment used in the experiments.[54]

Second, eq 3 was also applied to the diffusion of HDT on the HDT SAM. Averaging over all 18 data points in Figure 3(three temperatures and six concentrations), the average activation energy of diffusion (eq 3) per molecule in a 25 C16T molecule cluster on the C16T SAM is 15.6 $\pm$ 2.2 kJ mol$^{-1}$. This is approximately twice the 9 $\pm$ 1 kJ mol$^{-1}$ activation energy

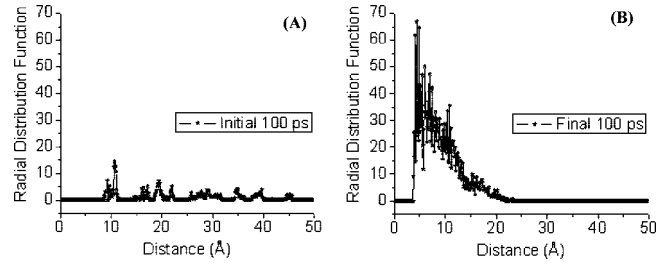


**Figure 5.** (A) Radial distribution functions (RDF) of the central carbon atom for seven hexadecanethiol molecules on a hexadecanethiol SAM at 270 K, for the first 100 ps of equilibration (restrained dynamics, as described in the text). (B) RDFs of the central carbon atom for seven hexadecanthiol molecules on a hexadecanethiol SAM at 270 K, for the final 100 ps of 1.8 ns of free dynamics.

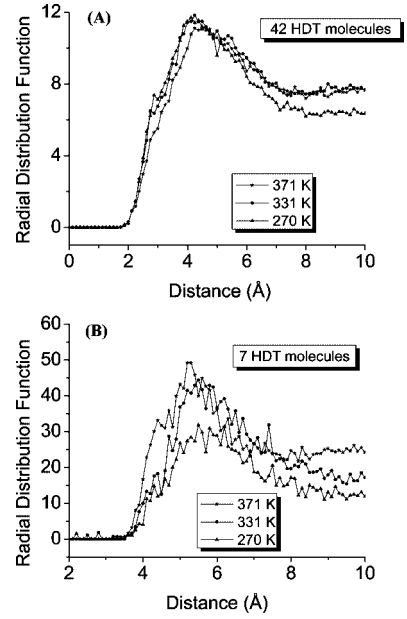


**Figure 6.** Radial distribution functions (RDF) of the central carbon atom for (A) 42 and (B) 7 hexadecanethiol molecules on a hexadecanethiol SAM at three different temperatures.

computed for one tricresyl phosphate molecule on a octadecyltrichlorosilane SAM,[32] reflecting the different nonbonded interactions occurring for the different molecule-on-SAM systems. As well as the different diffusing molecules and SAM types,[32] the $\mu$-CP simulation cells used in the present work feature molecule−molecule as well as molecule−SAM interactions, unlike ref 32.

*3.3.3. Structures of Ink Aggregates Formed on SAMs.* Having quantified ink diffusion on the SAM and estimated an energetic barrier to diffusion, we now turn to an analysis of the structure of the ink deposited on the SAM, describing in detail the concentration-dependent conformations. The ink molecules were placed initially in a lattice arrangement one molecule deep, flat onto the SAM. Figure 5A shows a radial distribution function (RDF) of the middle carbon atoms in a seven-molecule system at 270 K, during the first 100 ps of equilibration data when the ink molecules were restrained to their starting positions. The relatively flat distribution in Figure 5A demonstrates that the chains are isolated from each other initially. Figure 5B shows an RDF also of the middle carbon atoms but for the final 100 ps of free dynamics. In contrast to the "initial" distribution, the "final" distribution has only one broad peak, reflecting the aggregation of the ink molecules into clusters on the SAM surface. Likewise Figure 6 shows RDFs of the middle carbon atoms, but

(53) Supple, S.; Quirke, N. *Phys. Rev. Lett.* **2003**, *90*, 214501.
(54) Bain, C. D.; Troughton, E. B.; Tao, Y. T.; Evall, J.; Whitesides, G. M.; Nuzzo, R. G. *J. Am. Chem. Soc.* **1989**, *111*, 321–335.

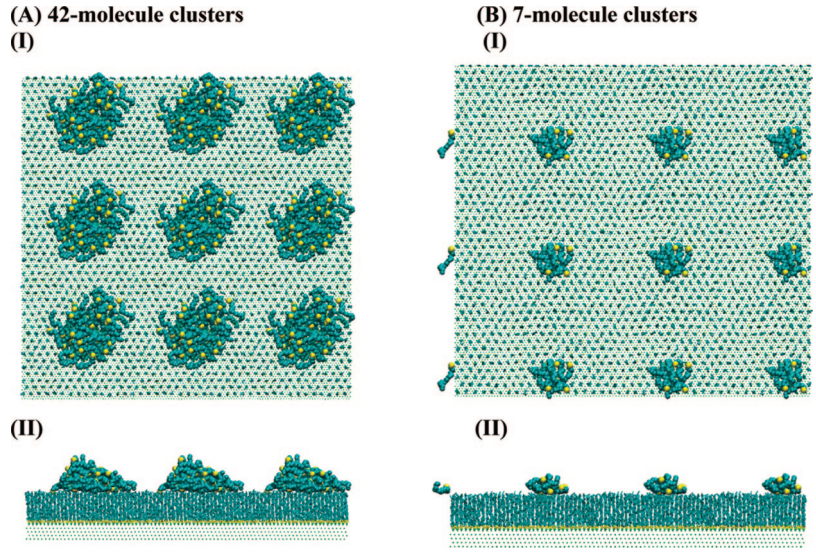


**Figure 7.** Final MD conformations of ink molecules over nine unit cells at 331 K, with concentrations of (A) 42 and (B) 7 hexadecanthiol molecules.

in this case over the entire 1.8 ns of free dynamics, with a comparison between high and low concentration arrangements, as described below.

Comparing panels A and B of Figure 6, we see that the peaks at the lower 7-molecule concentration (panel B), are approximately four times larger than those at the higher 42-molecule concentration. This is due to the increased density at the higher concentration. It is also seen that there is little temperature dependence in the clustering of the more concentrated 42-molecule arrangement, while the 7-molecule arrangement on the other hand shows a significant decrease in clustering at 371 K. This is interpreted as the 7-molecule ink clusters at 371 K being metastable and serves to explain the large standard deviation of the computed diffusion coefficient at low concentration and high temperature (Figure 3). However, even for such a small cluster at high temperature, no evaporation was observed over the course of the simulation. Figure 7 shows snapshots of the final conformations obtained at 331 K following 1.8 ns of free dynamics. The central periodic cell is surrounded by eight image cells giving a $3 \times 3$ matrix of cells. The aggregation demonstrated in Figure 6 and Figure 7 shows that the surface is autophobic,[55] in agreement with earlier computational studies carried out on the related hexadecane.[26] However, although the SAM surface is autophobic, the high diffusion coefficients show there is no nanoscale autophobic pinning,[49] as described above. Experimental testing of this prediction would be interesting but is outside the scope of the present work.

## 4. Conclusions

Experimental characterization techniques such as scanning electron microscopy provide a wealth of information on ink diffusion and pattern spreading in $\mu$-CP using alkanethiol SAMs on gold, allowing estimation of overall spreading rates and optimum stamp contact times under room temperature conditions. Theoretical work provides a valuable aid, allowing insight into the atom-scale features of ink spreading and calculation of ink diffusion rates, over a range of possible printing conditions. Indeed, this work has filled in some gaps in the experimental knowledge of $\mu$-CP materials and printing conditions. We have mapped out the range of diffusion coefficients for alkanethiol ink printing using hexadecanethiol SAMs, providing data for the identification of suitable ink concentrations and operating temperatures for a given $\mu$-CP application.

Our principal finding is that, while hexadecanethiol surfaces are autophobic, the autophobicity is not enough to pin the ink solutions on the SAM. Consequently any overinking of the SAM will lead to spreading of the printed pattern, with ink diffusion rates of approximately the same order of magnitude as bulk diffusion coefficients at all but the lowest surface concentrations and highest printing temperatures. Furthermore, comparison of computed ink-on-SAM diffusion coefficients with experimental diffusion rates supports an interpretation of pattern broadening in $\mu$-CP as a mixture of spreading on fully and partially formed SAMs.

**Acknowledgment.** This work was funded by the EC NaPa project (Contract No. NMP4-CT-2003-500120). Calculations were performed at Tyndall National Institute using computer resources provided by Science Foundation Ireland (SFI) and also at the SFI/HEA Irish Centre for High-End Computing (ICHEC). We thank Dr. Heiko Wolf and Professor Priya Vashishta for discussions.

**Supporting Information Available:** Additional figures and tables showing HDT tilt angles as a function of time, computed temperature depencence of SAM tilt angles, and overall diffusion coefficients at different temperatures for ranges of alkanethiols and HDT. This material is available free of charge via the Internet at http://pubs.acs.org.

LA802548U

(55) Zisman, W. A. *Ind. Eng. Chem.* **1963**, *55*, 19–38.